IEEE Access
Multidisciplinary | Rapid Review | Open Access Journal

Received 22 August 2024, accepted 9 September 2024, date of publication 16 September 2024, date of current version 7 October 2024.

Digital Object Identifier 10.1109/ACCESS.2024.3461324

RESEARCH ARTICLE

A Novel Fusion Technique for Early Detection of Alopecia Areata Using ResNet-50 and CRSHOG

HAIDER ALI KHAN AND SYED M. ADNAN
Department of Computer Science, University of Engineering and Technology at Taxila, Taxila 47050, Pakistan
Corresponding author: Syed M. Adnan (syed.adnan@uettaxila.edu.pk)

ABSTRACT Alopecia Areata is an autoimmune disorder where the body's immune system attacks normal cells instead of intruders, leading to hair loss. If not detected early, it can progress to complete scalp baldness (Alopecia Totalis) or total body hair loss (Alopecia Universalis). Therefore, early detection of Alopecia Areata is crucial. Computer vision and deep learning techniques have been used for the last few years in the field of dermatology to detect different relevant diseases. We proposed a robust feature fusion technique, named AlopeciaDet for the timely detection of Alopecia Areata using camera images instead of dermoscopic images that require specialized equipment. AlopeciaDet combines Corner Rhombus Shape HOG (CRSHOG) features with those extracted from the ResNet-50 pre-trained model to detect Alopecia Areata with high accuracy by using the Dermenet dataset. The geometric properties of rhombus shapes make them useful for recognizing patterns in an image. HOG captures local object appearance and shape by computing the distribution of intensity gradients in localized portions of the image. We combined these characteristics into CRSHOG. Alopecia Areata, on the other hand, is characterized by distinctive patterns and shapes of hair loss, with the most common feature being round or oval-shaped patches. These patches can vary in size and usually have well-defined, sharp edges. Consequently, our proposed CRSHOG significantly improves the extraction of local information from images of affected areas. It achieves this by integrating sign and magnitude data, thereby enhancing discrimination capabilities for texture classification tasks. Finally, the magnitudes and directions of these pixel values are calculated. We achieved an accuracy of 99.45% with an error rate of 0.55% using Artificial Neural Network. These results surpass the accuracy of current state-of-the-art techniques in this field.

INDEX TERMS Alopecia areata, feature extraction, features fusion, computer vision, deep learning, corner rhombus shape HOG (CRSHOG), ResNet-50.

I. INTRODUCTION

Hair significantly characterizes a person's appearance. It is essential not only for a positive self-image but also for protecting the scalp from harsh weather conditions. Scalp diseases can greatly affect hair health. Hair loss, while altering one's appearance, can also lead to emotional distress and even depression. Alopecia Areata, a disconcerting autoimmune disorder that causes hair loss, is the most prevalent disease. This illness manifests itself in clearly defined patterns, most frequently as round patches on the scalp or other body parts [1]. Millions of people worldwide are impacted by this disorder, which can be emotionally and physically upsetting. There are reports of 18.2% anxiety disorder and 8.8% serious depression in Alopecia Areata patients in comparison with 2.5% and 1.3-1.5% of the general population respectively [2]. It is observed that by the age of 70, hair loss may affect up to 80% of Caucasian men and up to 40% of Caucasian women. Planning a successful course of treatment for this illness requires an accurate and prompt diagnosis of the disease [3], [4].

The bald scalp's state is carefully evaluated using conventional methods. These tests may raise questions about the accuracy of the diagnosis and the condition of the scalp because they rely on the knowledge of dermatologists and other pertinent professionals [5]. Significant progress has

The associate editor coordinating the review of this manuscript and approving it for publication was Chao Zuo.

been made in the field of medical image analysis research due to the latest developments in computer vision and deep learning techniques [6]. Combining these techniques has demonstrated significant potential in automating the identification and classification of different dermatological conditions [7]. Apart from conventional diagnosis, Alopecia Areata is extremely difficult to diagnose, leading to several difficulties.

The following are the main technological obstacles that need to be overcome when using computer vision and machine learning techniques for the early detection of Alopecia Areata:

1. **Image Quality and Standardization**: Sustaining constant image quality across a wide range of devices and scenarios is essential for trustworthy analysis. Adjustments to the illumination, resolution, and camera settings can affect the accuracy of computer vision algorithms [8].
2. **Feature Extraction**: Extracting relevant information from scalp images to differentiate between normal hair and early symptoms of Alopecia Areata can be difficult. Algorithms must be able to identify the minute differences in hair density, texture, and distribution [9].
3. **Variability in Conditions**: Among various patterns, Alopecia Areata can manifest as widespread thinning, patchy hair loss, or complete baldness. Computer vision models need to be sufficiently robust to accurately distinguish and categorize these different conditions [10].
4. **Data Labeling and Annotation**: To train computer vision algorithms, a sizable dataset of labeled scalp images is required. However, it may be subjective to appropriately annotate images for Alopecia Areata; consensus and expert opinion are required [11].
5. **Model Generalization**: Machine Learning models trained on a single dataset may perform incorrectly. Models need to be able to generalize across a range of patient demographics to be widely used [12].
6. **Real-time Analysis**: Real-time analysis of scalp images for early indications of Alopecia Areata is required in clinical settings to enable timely diagnosis and treatment. The development of efficient algorithms that can quickly interpret images without compromising accuracy is another technical challenge [8].
7. **Ethical Considerations**: The privacy concerns of patients while collecting and processing images must be considered. Obtaining patients' consent and implementing secure data protection mechanisms are crucial ethical considerations [13].

Dermatologists, technological experts, and other medical professionals need to collaborate to address these technological challenges. Furthermore, for reliable and accurate early detection of Alopecia Areata, computer vision algorithms need to be enhanced and more optimized.

To address the problem of early detection and classification of Alopecia Areata, our proposed research study thoroughly examines the creative integration of deep learning and computer vision techniques. In this work, we propose a novel features fusion technique AlopeciaDet: features from ResNet-50 and CRSHOG, the variant of Histogram of Oriented Gradients (HOG) [14], are combined. This proposed technique provides enhanced accuracy and reliability in the diagnostic process. By combining the advantages of these two cutting-edge algorithms, this research offers a reliable and accurate response to a critical dermatological issue.

Combining extracted data from CRSHOG and ResNet-50 presents a novel way to take advantage of their complementary strengths, which enhances the identification and classification of Alopecia Areata. Using the idea of transfer learning, the final system gains from the information acquired by the ResNet-50 pre-trained model, which is trained on the large image repository of the Imagenet dataset [15]. The following are the key contributions of our proposed AlopeciaDet:

1. Developed a cost-effective technique to detect and classify Alopecia Areata more accurately from camera images rather than dermoscopic images, which requires highly sophisticated equipment and professional staff to operate.
2. We have proposed an improved version of HOG the CRSHOG, which extracts more precise features.
3. As far as early detection and classification from camera images are concerned, they generally lack in terms of accuracy due to comparatively low definition. However, we have achieved a promising accuracy of 99.45% with the novel fusion of features generated from CRSHOG and ResNet-50 in our proposed AlopeciaDet.

The remaining portions of the document are organized as follows:

Section II presents examples from the relevant literature, whereas Section III concentrates on the suggested methodology. Section IV presents the results and comparison with the most recent methods. Section V provides the conclusion.

II. RELATED LITERATURE

Hair loss problems can be examined in a variety of ways, including:

A. FROM DERMOSCOPIC IMAGES

Visual inspection is used in conjunction with microscopic techniques to diagnose hair loss with its severity and other scalp diseases. Alopecia Areata is diagnosed using both deep learning and classical machine learning methods. Olsen and Canfield determined the hair density and the percentage of hair loss using the Severity of Alopecia Tool (SALT) [16]. To get the overall percentage of scalp hair loss, the percentage of hair loss in each quadrant is determined, multiplied by the total area of the scalp that each quadrant represents, and the results are added for each quadrant. The intricate and challenging-to-generalize scoring approach could affect scoring reproducibility. Nevertheless, monitoring the progression of the disease and the effectiveness of treatment depends on the assessment's repeatability. To accomplish this, a hair

specialist annotated a dataset of 100 images from young patients suffering from Alopecia Areata. And classify alopecia areas in various ways including normal density, scalp, clinically scalp, low-density hair patches, and hair partition. Bernardis and Castelo-Soccio developed an algorithm to differentiate between bald and normal scalp regions. It can also identify regions with low hair density [17]. AloNet deep learning architecture was introduced by Lee et al. as a means of measuring Alopecia Areata. For training, a dataset including 2000 images of individuals with Alopecia Areata was utilized. A dermatologist annotated the dataset. Eight dermatologists assessed 400 images for testing [18]. Reference [19] only employed Lead-II ECG images to differentiate between abnormal heartbeats, COVID-19, myocardial infarction, and normal sinus rhythm. With AlexNet, the researchers were able to achieve an accuracy of 77.42%, and with VGG19, they were able to achieve 75% accuracy. Using feedforward and backpropagation neural networks, Kapoor and Mishra devised a method to diagnose Alopecia Areata early and achieved 91.00% accuracy [3]. Grid line selection and eigenvalues are two techniques that Seo and Park suggested utilizing to process scalp images to identify information related to hair loss using Trichoscopy [20].

B. FROM CAMERA IMAGES

To identify female pattern hair loss (FPHL), which is usually detected by eye inspection and the Ludwig and Savin scales, Hung et al. used a method to assess the balding area. In this research, images of 33 women with FPHL were analyzed using Principal Component Analysis. The values of Balding Width (BW) and the hair loss grades on the Savin scale showed a strong association [20], [21], [22].

Using a webcam and microscope camera sensors to capture crown pictures, Lee and Yang extracted binary images using the Otsu threshold value [24]. Next, the binary image is subjected to two applications of the K-means clustering algorithm: the first time, $k = 4$ is used to segment the background environment and hair, and the second time, $k = 2$ is used to segment the image's non-hair and hair components. The Hamilton-Norwood scale is used to measure the baldness stage during the detection process [25] and achieved an accuracy of 51.00-95.00%. 675 images were classified by Benhabiles et al. using a method for identifying male pattern baldness in facial images. The average accuracy of this algorithm, which used the Hamilton-Norwood scale, was 82.00-86.00% [26].

Instead of using dermoscopic images, Shakeel et al. suggested a method to identify and categorize Alopecia Areata from camera images. In the image preprocessing stage, researchers used histogram equalization to enhance the image quality. Following that, the edge detection technique was used to obtain the Region of Interest (ROI) in the image segmentation phase. Then the ROI's shape, color, and texture features were extracted. In the end, SVM and KNN classifiers were used to classify the features vector, yielding results of 91.40% and 88.90% respectively. Although this helped to identify and categorize Alopecia Areata from typical camera images, the accuracy was not remarkable [27].

Rai et al. suggested a deep learning-based method for the identification of Alopecia Areata to close this gap. For feature extraction, SqueezeNet, VGG-16, VGG-19, and Inception-V3 pre-trained models were used. The dataset was divided into 70% for training and 30% for testing by the researchers in a 7:3 ratio. After that, the data was sent to the ANN, SVM, and Logistic Regression classifiers, and achieved a 98.30% accuracy rate. Although researchers achieved higher accuracy, they used a dataset that is not publicly available [28]. In 2022, Aditya et al. presented a method utilizing CNN that could identify and categorize Alopecia Areata from typical camera images with 92% accuracy [29].

Faster Residual Convolutional Neural Network (FRCNN) was the method for Alopecia Areata detection and classification that C. Saraswathi and B. Pushpa proposed in 2023; they achieved 84.30% accuracy. In their second research investigation, researchers used the Modified Extreme Learning Machine (MELM) algorithm to achieve 92.64% accuracy [30], [31]. With 98% accuracy, Mittal et al.'s CNN-based method for identifying Alopecia Areata was proposed. Using an SVM classifier, Shabnam and Farook Sayyad's technique—which included the properties of CNN and VGG—achieved 98% accuracy [32], [33]. A summary of techniques for the detection of Alopecia Areata from normal camera images is shown in Table 1.

TABLE 1. Classification accuracies of existing techniques for the detection of alopecia areata.

Ref.	Year	Dataset	Feature Ext.Tech.	Classifier	Accuracy (%)
[27]	2021	Figaro1K, Dermnet	Shape, Color, Texture features	SVM	91.40
[28]	2021	Own Dataset	VGG16,VGG19,Inception V3	ANN, Logistic Regression, SVM	98.30
[29]	2022	Figaro1K, Dermnet	CNN	CNN	92.00
[30]	2023	Dermnet	FRCNN	FRCNN	84.30
[31]	2023	Dermnet	Shape, Color, Texture features	MELM	92.64
[32]	2023	Dermnet	CNN	CNN	98.00
[33]	2023	Figaro1k, Dermnet	VGG, CNN	SVM	98.00

The literature study above makes it abundantly evident that dermoscopic images taken with appropriate equipment are required for the clinical diagnosis of Alopecia Areata. It also

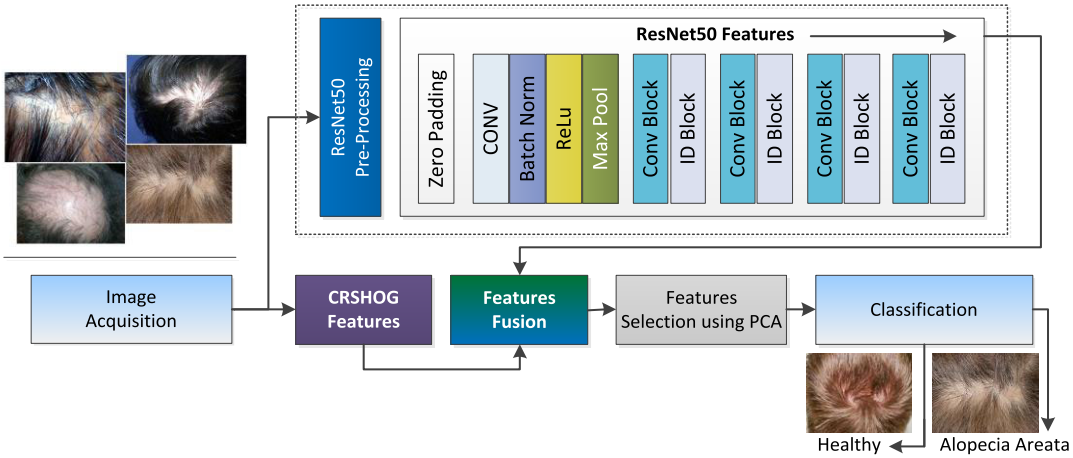

FIGURE 1. Proposed alopeciadet block diagram for the early detection and classification of alopecia areata.

needs qualified personnel to run the specialized machinery. However, the diagnosis of Alopecia Areata with standard camera images of scalp hair is less expensive and easier for casual staff to handle in terms of patient imagery. Though a maximum of 98.30% accuracy has been achieved by Rai et al. [28], the paradigm of the proposed AlopeciaDet framework using CRSHOG and ResNet-50 is more productive. AlopeciaDet has achieved a remarkable accuracy of 99.45% in comparison with other state-of-the-art techniques used in this research area.

III. PROPOSED METHODOLOGY

We have proposed a novel, reliable, and robust technique AlopeciaDet for the early detection and classification of Alopecia Areata.

We utilized ResNet50 with input dimensions of 224 × 224 and output feature dimensions of 7 × 7 ×2048. For CRSHOG features, we employed a 9-bin histogram for normalizing 16×16 blocks. Concatenating these features yielded a 36 × 1 element vector, with 16 × 16 blocks moving across 105 positions (7 horizontal and 15 vertical positions on an image sized 64 × 128), resulting in a total dimensional vector size of 3780. Regarding PCA, we retained 50 principal components. The proposed methodology is shown in Figure 1.

The novel methodology is based on our improved Corner Rhombus Shape HOG (CRSHOG) and ResNet-50.

A. RESNET-50

ResNet-50, a Residual Network with 50 layers, is known for using residual learning [34]. The main contribution of ResNet-50 is the introduction of residual blocks, which solve the vanishing gradient problem and enable the training of much deeper networks. The model's mathematical representation is as follows:

1. Residual Block: A residual block is made up of multiple layers, where the block's input is added straight to the output. This has the following mathematical expression:

$$V_y = F(V_x, \{Wt_i\}) + V_x \tag{1}$$

where:

- Vx is the input to the block.
- Vy is the output of the block.
- $F(Vx, \{Wt_i\})$ stands for the residual function (for example batch normalization, ReLU activations, and a stack of convolutional layers) with parameters $\{Wt_i\}$.

More specifically, the formulation of a residual block with two convolutional layers is as follows:

$$V_y = \sigma(Wt_j \cdot \sigma(Wt_i \cdot V_x + b_i) + b_j) + V_x \tag{2}$$

where:

- Wt_i and Wt_j are the weight matrices of the convolutional layers.
- b_i and b_j are the bias terms.
- σ denotes the activation function, typically ReLU.

2. Bottleneck Residual Block: The bottleneck block, which has three layers, is a unique kind of residual block used by ResNet-50 as shown in Equation 3.

$$V_y = Wt_k \cdot \sigma(Wt_j \cdot \sigma(Wti \cdot V_x + bi) + b_j) + b_k + V_x \tag{3}$$

where:

- Wt_i is a 1 × 1 convolution reducing the dimension.
- Wt_j is a 3 × 3 convolution.
- Wt_k is a 1 × 1 convolution restoring the dimension.
- σ denotes the activation function, typically ReLU.

3. Network Architecture: ResNet-50 is comprised of a sequence of residual blocks that come after the first convolutional layer.
4. Forward Pass: During the forward pass through the network, each layer and residual block are applied in turn as shown in Equation 4.

$$V_y = Softmax(Wt_{fc} \cdot AvgPool(R_5) + b_{fc}) \tag{4}$$

where $R5$ is the last residual block stage's output. *Wtfc* and *bfc* are the weights and biases of the fully connected layer.

Using ResNet-50 for feature extraction in the detection and classification of Alopecia Areata from hair images offers several benefits:

1. ResNet-50 is a deep convolutional neural network (CNN) architecture that can recognize hierarchical characteristics in images, allowing it to capture complicated patterns with ease [15].
2. Due to its training on large datasets such as ImageNet, the pre-trained ResNet-50 model can be enhanced on smaller datasets containing hair images relevant to Alopecia Areata. This method reduces the requirement for large labeled datasets and processing resources by utilizing the transfer learning concept [35].
3. ResNet-50 has been shown to perform better in a range of image recognition applications because of its batch normalization layers, skip connections, and depth. The accuracy with which this architecture recognizes and classifies patterns associated with Alopecia Areata is remarkable [36].
4. ResNet-50 exhibits resilience in the face of alterations in visual conditions, such as lighting, orientation, and background clutter. Maintaining constant performance in real-world scenarios when working with multiple sets of hair images collected under different conditions requires this robustness [37].
5. The hierarchical structure of ResNet-50's learned properties lends them some interpretability. Examining the activations of multiple layers can help to identify the features that are most crucial to the model's decision-making process [38].
6. ResNet-50 performs better in terms of computing efficiency than deeper topologies like ResNet-101 or ResNet-152. Large-scale or real-time applications can gain from faster inference times due to their scalability [39].
7. ResNet-50 is still one of the most sophisticated CNN architectures available for image classification applications. Its efficacy has been extensively examined and confirmed in several domains, including medical image analysis [40].

Furthermore, as ResNet-50 won the 2015 ILSVRC ImageNet competition, it was selected as the base model [41] and thus is helpful for disease identification and classification in medical image analysis studies [42].

B. CORNER RHOMBUS SHAPE HOG (CRSHOG)

In this proposed algorithm, a mask of 4×4 is applied to the image. As shown in Figure 2 the average of the left two corners and right two corners is performed to calculate $g_x Corner$ by using the following equation.

$$g_x Corner(x, y) = I(x + 1, y) - I(x - 1, y) \tag{5}$$

Similarly, the average of the top two corners and bottom two corners is performed to calculate $g_y Corner$ by using the following equation.

$$g_y Corner(x, y) = I(x, y + 1) - I(x, y - 1) \tag{6}$$

Then, the average of the left rhombus rib and right rhombus rib is calculated to obtain $g_x Rhombus$. Similarly, the average of the top rhombus rib and bottom rhombus rib is calculated to obtain *gyRhombus*. Then the average of *gxCorner* and *gxRhombus* is calculated to obtain gx and the average of *gyCorner* and *gyRhombus* is calculated to obtain gy. Finally, the Gradient magnitude (g) and Gradient direction (θ) are calculated by using the following equations 7 and 8.

$$Gradient\ magnitude(g) = \sqrt{g_x^2 + g_y^2} \tag{7}$$

$$Gradient\ Direction(\theta) = arctan\left[\frac{g_y}{g_x}\right] \tag{8}$$

The next step is to create a histogram of gradients. The histogram contains 9 bins, each bin is of 20^0. Here the numbers representing the gradients and the angles are between 0^0 and 180^0. Since the values for a gradient and its negative are the same, we only considered unsigned gradients. To put it another way, because of its vertical direction, a gradient arrow to 90^0 opposite it for -270^0 is regarded as the same.

In Figure 3, the procedure for choosing bins and the histogram based on magnitudes against θ values for the voting directions for each bin are shown. In the magnitude matrix, the value that corresponds to the specific value from gradient direction 60^o is 22. Since the gradient direction is exactly equal to bin number 3 for the value of 60^0, the magnitude 22 is placed in this bin. Otherwise, the higher contribution should be to the bin value, which is closer to the orientation. Using Equations 9 and 10, we can determine the values for both proportions.

$$V_j = m\left[\frac{Bin_{j+1} - \theta}{\Delta\theta}\right] \tag{9}$$

$$V_{j+1} = \mu\left[\frac{\theta - Bin_j}{\Delta\theta}\right] \tag{10}$$

Here, $\theta = \frac{180^o}{9} = 20^o$, C_J is the value of J^{th} bin and $m =$ magnitude. The nine-bin histogram is produced by adding the contributions of each pixel in the resulting matrix.

Figure 3 shows the computation of CRSHOG on an image of Alopecia Areata.

Figure 4 shows the original image, and visualization of HOG and CRSHOG magnitude to see the difference between the effect of applying HOG and our proposed CRSHOG. There is a clear difference between HOG and CRSHOG magnitude.

The features extracted from CRSHOG and ResNet-50 are combined and then Principal Component Analysis (PCA) is applied. There are some key motivations for using PCA for the best selection of features from our combined large feature set. PCA preserves most of the original variance in

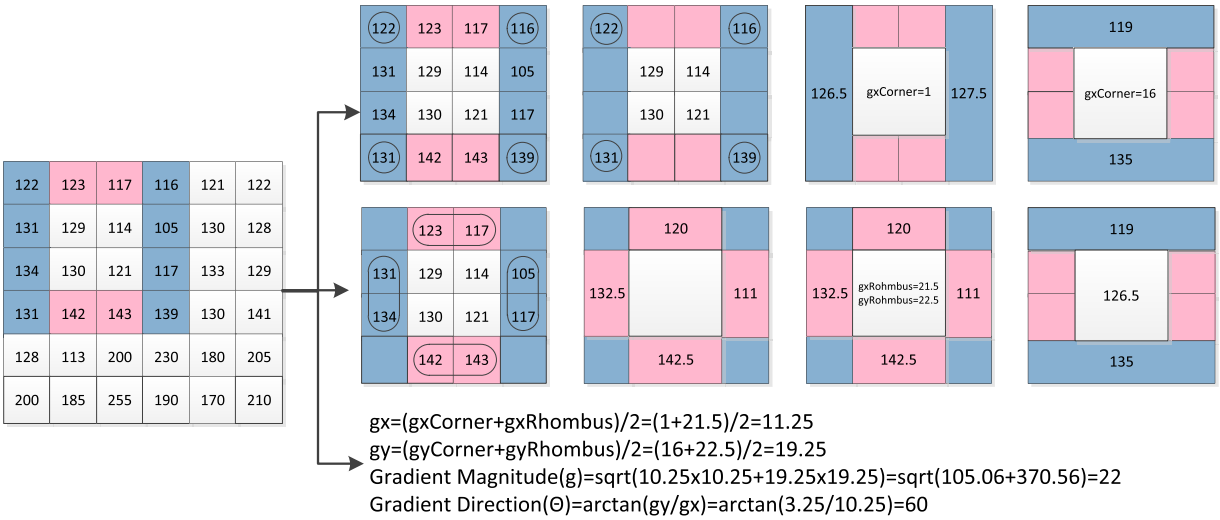

FIGURE 2. Calculation of gradient magnitude and gradient direction for the proposed CRSHOG.

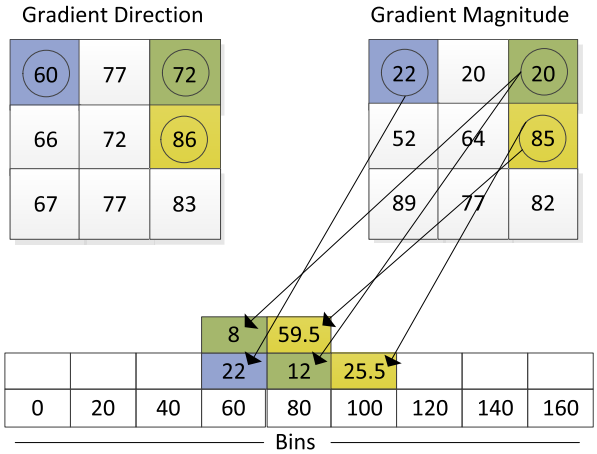

FIGURE 3. CRSHOG-based histogram of gradients.

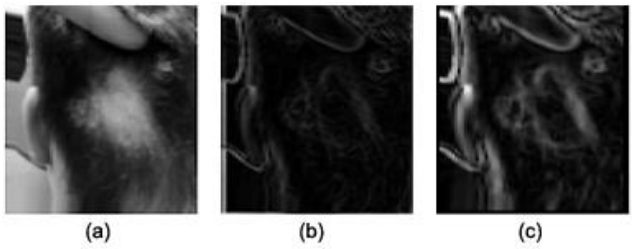

FIGURE 4. Gradient magnitude of an image affected by alopecia areata (a) Original image (b) HOG Magnitude (c) CRSHOG Magnitude.

a dataset while reducing the number of features. It simplifies the model by reducing the original features to a smaller set of uncorrelated components while retaining substantial information. It efficiently filters away components that are of less significant variations in the data by concentrating on the principal components that capture the greatest variance [41], [42].

These features can be visualized by using SHAP values as shown in Figure 5.

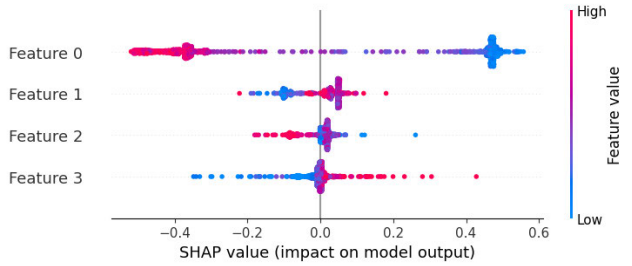

FIGURE 5. SHAP value-based visualization of selected features after applying PCA.

Algorithm 1 Algorithm of AlopeciaDet for Early Detection and Classification of Alopecia Areata.

Input: Scalp image.
Output: Alopecia Areata/Healthy.
1. Read image.
2. Conversion of the image to grayscale.
3. Extract the features using the proposed CRSHOG and make the histogram.
4. Extract the features using ResNet-50.
5. Apply fusion of both feature sets.
6. Apply PCA for feature selection.
7. Apply different classifiers for the classification of Alopecia Areata.

C. ALGORITHM

The complete algorithm of the proposed technique is given below.

IV. EXPERIMENTATION METHODS AND RESULTS

A. DATASET USED

The healthy hair images are retrieved from the Figaro 1K dataset [45]. There are a total of 811 healthy hair images. As far as the images of Alopecia Areata are concerned, they

are retrieved from the Dermnet dataset from Kaggle [46]. There is a total of 71 images of Alopecia Areata. We used data augmentation to address the problem of overfitting, which is prevalent when training sophisticated models with small samples. Generating synthetic samples from the available training data improves the generalization capacity of the model. The standard augmentation approaches [47], commonly used in the literature to improve performance, is employed in this work. Although there are many methods for creating new images from pre-existing training samples, we concentrated on the most widely used ones, which include rotation, and horizontal and vertical mirroring. The dataset was augmented using these common augmentation methods.

We combined the Figaro1K for healthy images and augmented Alopecia Areata images, named as Figaro-Dermnet dataset. The sample images are shown in Figure 6.

B. ENVIRONMENTAL SETUP

To evaluate the performance of classifiers, Precision, Recall, F1-Score, Accuracy, and Error Rate have been calculated for SVM, Random Forest, Decision Tree, Naive Bayes, Logistic Regression, and KNN classifiers. Finally, the proposed AlopeciaDet is compared to existing techniques to show its effectiveness.

Precision gives us the measure that how correctly we are identifying a class, out of all predicted as a positive class i.e. True Positive (TP) + False Positive (FP). It can be calculated by using Equation 11. Recall is the measure of how the model is correctly predicting the class out of truly predicted (TP) + true class predicted as a negative class i.e. False Negative (FN). It can be calculated by using Equation 12. To identify the classifier's average precision and recall, the F-1 Score is calculated using Equation 13.

Accuracy is the ratio between the correct predictions and the total predictions by the classifier as shown in Equation 14. As far as the Error rate is concerned, it is the ratio between total false predictions i.e. (FP + FN), and all the predictions by the classifier as shown in Equation 15.

$$Precision = \frac{TP}{TP + FP} \tag{11}$$

$$Recall = \frac{TP}{TP + FN} \tag{12}$$

$$F1 - Score = 2 \times \frac{\text{Precision} * Recall}{\text{Precision} + Recall} \tag{13}$$

$$Accuracy = \frac{TP + TN}{TotalPositive + TotalNegative} \tag{14}$$

$$ErrorRate = \frac{FP + FN}{TotalPositive + TotalNegative} \tag{15}$$

We have performed all the experiments in Python by using Google Colab, while the images are uploaded on Google Drive, divided into two classes: Alopecia Areata and Healthy as mentioned earlier. Precision, Recall, Accuracy, and F1-Score are calculated for the classifiers Decision Tree, Random Forest, Naive Bayes, SVM, KNN, Logistic Regression, and Neural Network as shown in Table 2.

FIGURE 6. (a) Dermnet dataset sample images of alopecia areata. (b) Figaro 1K dataset sample images of healthy hair.

TABLE 2. Performance metrics summary of proposed AlopeciaDet using different classifiers on the Figaro- Dermnet dataset.

Classifier	Class	Prec. (%)	Recall (%)	F1-Score (%)	Accuracy (%)
Random Forest	Alopecia Areata	99.35	98.70	99.02	98.89
	Healthy	98.31	99.15	98.72	
Decision Tree	Alopecia Areata	99.02	98.38	98.70	98.52
	Healthy	97.88	98.72	98.30	
SVM	Alopecia Areata	99.67	99.03	99.35	**99.26**
	Healthy	98.73	99.57	99.15	
GNB	Alopecia Areata	97.44	98.70	98.06	97.79
	Healthy	98.26	96.58	97.41	
Logistic Regression	Alopecia Areata	99.67	99.03	99.35	**99.26**
	Healthy	98.73	99.57	99.15	
KNN	Alopecia Areata	100.00	98.70	99.35	**99.26**
	Healthy	98.32	100.0	99.15	
ANN	Alopecia Areata	99.67	99.35	99.51	**99.45**
	Healthy	99.15	99.57	99.36	

Moreover, the True Positive Rate (TPR) and True Negative Rate (TNR) are high, on the other hand, False Positive Rate (FPR) and False Negative Rate (FNR) are low as shown in Table 3. Tables 2 and 3 show the excellent classification performance of the proposed method. Figure 7 shows the ROC curve for the Artificial Neural Network classifier by using the Adam optimizer with a default learning rate of 0.001 and batch size of 64.

Figures 8 and 9 show the training and testing accuracy and loss curves on the graph, which clearly show the very good performance of the model and have very little loss. Figure 10

TABLE 3. Classification performance of proposed AlopeciaDet using different classifiers on the Figaro- Dermnet dataset.

Classifier	TPR (%)	TNR (%)	FPR (%)	FNR (%)	Error rate (%)
Random Forest	99.00	99.00	1.00	1.00	1.11
Decision Tree	99.00	98.00	2.00	1.00	1.48
SVM	**100.00**	**99.00**	**1.00**	**0.00**	**0.74**
GNB	97.00	99.00	1.00	3.00	2.21
Logistic Regression	**100.00**	**99.00**	**1.00**	**0.00**	**0.74**
KNN	**100.00**	**99.00**	**1.00**	**0.00**	**0.74**
ANN	**100.00**	**99.00**	**1.00**	**0.00**	**0.55**

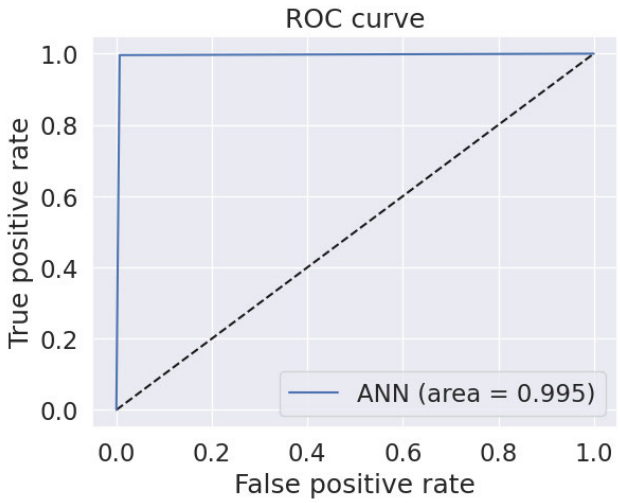

FIGURE 7. ROC curve showing the performance of the artificial neural network.

shows the average values of Precision, Recall, F1-Score, and accuracy using different classifiers. The graph represents the maximum values 99.41%, 99.46%, 99.44%, and 99.45% of Precision, Recall, F1-Score, and Accuracy respectively using ANN.

C. VALIDATION

The proposed technique was validated on another dataset named Hair Diseases. There are a total of 10 hair diseases and in each disease folder, there are 960 images. Therefore, for Alopecia Areata, there are 960 images [48].

Precision, Recall, F1-Score, and Accuracy are validated for three models trained using SVM, KNN, and ANN, as shown in Table 4. A validation accuracy of 96.62% has been achieved from the model trained by using the ANN classifier.

Similarly, TPR, TNR, FPR, and FNR are shown in Table 5.

D. COMPARISON WITH RESNET-50 PRE-TRAINED MODEL

We compared AlopeciaDet with ResNet-50 on the same dataset Figaro-Dermnet. Precision, Recall, F1-Score, and Accuracy are calculated for the models trained using SVM,

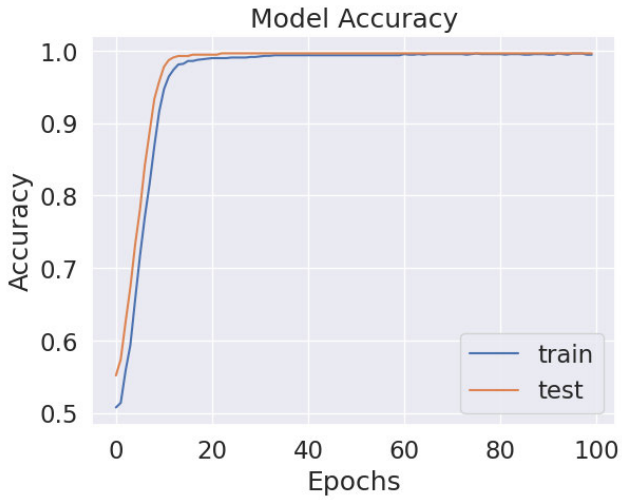

FIGURE 8. Accuracy curve for training and testing.

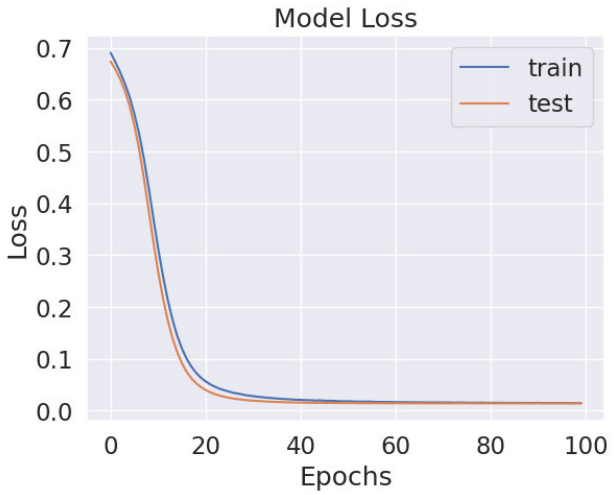

FIGURE 9. Loss curve for training and testing.

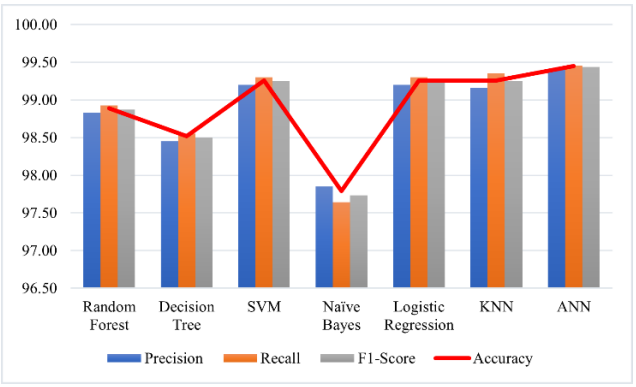

FIGURE 10. Average values of performance evaluation parameters using different classifiers.

Random Forest, Decision Tree, Naive Bayes, Logistic Regression, KNN, and ANN as shown in Table 6.

From Table 6, it is evident that the maximum accuracy achieved by using ResNet-50 is 98.34% with SVM

TABLE 4. Performance metrics summary of proposed AlopeciaDet using different classifiers validated on the hair diseases dataset.

Classifier	Class	Prec. (%)	Recall (%)	F1-Score (%)	Accuracy (%)
SVM	Alopecia Areata	97.19	96.58	96.88	96.24
	Healthy	94.81	95.71	95.26	
KNN	Alopecia Areata	96.88	96.58	96.73	96.05
	Healthy	94.79	95.24	95.01	
ANN	Alopecia Areata	95.51	99.07	97.26	**96.62**
	Healthy	98.48	92.86	95.59	

TABLE 5. Classification performance of proposed AlopeciaDet using different classifiers validated on the Hair Diseases dataset.

Classifier	TPR (%)	TNR (%)	FPR (%)	FNR (%)	Error rate (%)
SVM	96.00	97.00	3.00	4.00	3.76
KNN	95.00	97.00	3.00	5.00	3.95
ANN	93.00	99.00	1.00	7.00	3.38

TABLE 6. Performance metrics summary of ResNet-50 using different classifiers on the Figaro- Dermnet dataset.

Classifier	Class	Prec. (%)	Recal l (%)	F1-Score (%)	Accuracy (%)
Random Forest	Alopecia Areata	98.26	97.92	98.09	97.97
	Healthy	97.65	98.03	97.84	
Decision Tree	Alopecia Areata	96.90	97.57	97.23	97.05
	Healthy	97.22	96.46	96.84	
SVM	Alopecia Areata	99.29	97.57	98.42	**98.34**
	Healthy	97.30	99.21	98.25	
GNB	Alopecia Areata	95.59	97.92	96.74	96.49
	Healthy	97.57	94.88	96.21	
Logistic Regression	Alopecia Areata	99.29	97.57	98.42	**98.34**
	Healthy	97.30	99.21	98.25	
KNN	Alopecia Areata	99.29	96.88	98.07	97.97
	Healthy	96.55	99.21	97.86	
ANN	Alopecia Areata	98.94	97.22	98.07	97.97
	Healthy	96.91	98.82	97.86	

and Logistic Regression classifiers, while AlopeciaDet has achieved 99.45% with Artificial Neural Network and 99.26% with SVM, Logistic Regression and KNN classifiers.

E. COMPARISON OF ALOPECIADET WITH RESNET-50 AND HOG FEATURES

We compared AlopeciaDet with the features obtained by ResNet-50 and HOG on the same dataset Figaro-Dermnet. Precision, Recall, F1-Score, and Accuracy are calculated for the models trained using SVM, Random Forest, Decision Tree, Naive Bayes, Logistic Regression, KNN, and ANN as shown in Table 7.

TABLE 7. Performance metrics summary of Resnet-50 with hog using different classifiers on the Figaro-Dermnet dataset.

Classifier	Class	Prec. (%)	Recall (%)	F1-Score (%)	Accuracy (%)
Random Forest	Alopecia Areata	98.68	98.68	98.68	98.52
	Healthy	98.32	98.32	98.32	
Decision Tree	Alopecia Areata	98.36	98.68	98.52	98.34
	Healthy	98.31	97.90	98.11	
SVM	Alopecia Areata	99.67	98.36	99.01	**98.89**
	Healthy	97.93	99.58	98.75	
GNB	Alopecia Areata	98.36	98.36	98.36	98.15
	Healthy	97.90	97.90	97.90	
Logistic Regression	Alopecia Areata	99.67	98.36	99.01	**98.89**
	Healthy	97.93	99.58	98.75	
KNN	Alopecia Areata	99.66	97.70	98.67	98.52
	Healthy	97.13	99.58	98.34	
ANN	Alopecia Areata	99.34	99.01	99.18	**99.08**
	Healthy	98.74	99.16	98.95	

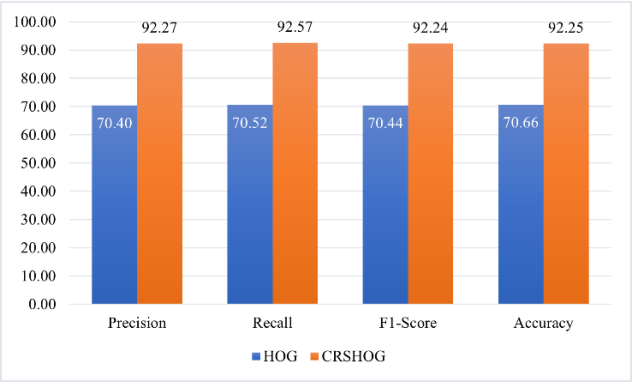

FIGURE 11. Comparison of performance evaluation parameters between CRSHOG and HOG using ANN classifier on the Figaro-Dermnet Dataset.

Table 2 and Table 7 show the clear difference between the proposed AlopeciaDet and the results obtained by extracting features using ResNet-50 and HOG.

F. COMPARISON BETWEEN CRSHOG AND HOG FEATURES

We have also generated results by applying HOG and our proposed CRSHOG feature descriptors and ANN classifier by using Adam optimizer with a default learning rate of 0.001 and batch size of 64 on the same dataset Figaro-Dermnet. Figure 11 shows the comparison between the two feature descriptor algorithms. We can see a clear difference between their performance.

G. COMPARISON WITH TECHNIQUES IN RELATED LITERATURE

Figure 12 shows the comparison between AlopeciaDet and the state-of-the-art techniques in related literature.

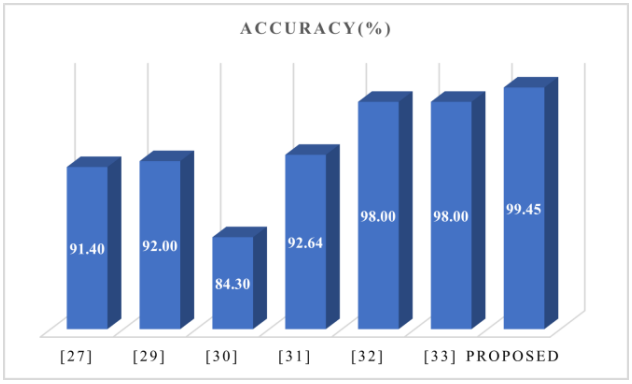

FIGURE 12. Accuracy comparison of proposed AlopeciaDet with state-of-the-art techniques.

V. CONCLUSION

We proposed AlopeciaDet, a novel feature fusion technique designed for the timely detection of Alopecia Areata using standard camera images rather than dermoscopic images that need specialized equipment. AlopeciaDet combined our proposed Corner Rhombus Shape HOG (CRSHOG) features with those derived from the ResNet-50 pre-trained model and achieved an accuracy of 99.45% by using the ANN classifier. For future work, our technique, AlopeciaDet, can be applied to dermoscopic images as well. Since our proposed method, CRSHOG is an enhanced version of the Histogram of Oriented Gradients and incorporates features from ResNet-50, this innovative fusion can potentially be generalized to address other dermatological conditions, such as various skin-related diseases.

STATEMENTS AND DECLARATIONS

- **COMPETING INTERESTS**

There are no conflicts of interest to declare.

- **AUTHORS' CONTRIBUTION STATEMENT**

The study and writing of this work were equally contributed to by its authors, Haider Ali Khan and Syed M. Adnan. Particularly, the two authors contributed to the conception of the study, experiment design, data analysis, and paper writing and revision.

- **ETHICAL AND INFORMED CONSENT FOR DATA USED**

Ethical Considerations: The Figaro 1K, Dermnet, and Hair Diseases datasets used in this research are obtained from publicly available datasets. There is no personally identifiable information collected or used. Throughout the research process, we followed the relevant ethical guidelines to protect the privacy and confidentiality of the people whose images are already included in the datasets.

- **DATA AVAILABILITY AND ACCESS**

The particular datasets utilized in this research are the Hair Diseases, Figaro 1K, and Dermnet datasets, all of which are openly accessible at:

https://www.kaggle.com/datasets/shubhamgoel27/dermnet

http://projects.i-ctm.eu/it/progetto/figaro-1k

https://www.kaggle.com/datasets/sundarannamalai/ hair diseases

REFERENCES

[1] K. Bhargava, D. Fenton, J. Chambers, and J. Tomlinson, "Alopecia areata and its impact on young people," *Dermatol. Nurs.*, vol. 14, no. 1, pp. 24–31, 2015.

[2] M. Miteva and A. Villasante, "Epidemiology and burden of alopecia areata: A systematic review," *Clin., Cosmetic Investigational Dermatol.*, p. 397, Jul. 2015, doi: 10.2147/ccid.s53985.

[3] I. Kapoor and A. Mishra, "Automated classification method for early diagnosis of alopecia using machine learning," *Proc. Comput. Sci.*, vol. 132, pp. 437–443, Jan. 2018, doi: 10.1016/j.procs.2018.05.157.

[4] A. Egger, M. Tomic-Canic, and A. Tosti, "Advances in stem cell-based therapy for hair loss," Tech. Rep., 2020.

[5] M. Sreenatha and P. B. Mallikarjuna, "A fault diagnosis technique for wind turbine gearbox: An approach using optimized BLSTM neural network with undercomplete autoencoder," *Eng., Technol. Appl. Sci. Res.*, vol. 13, no. 1, pp. 10170–10174, Feb. 2023, doi: 10.48084/etasr.5595.

[6] M. Puttagunta and S. Ravi, "Medical image analysis based on deep learning approach," *Multimedia Tools Appl.*, vol. 80, pp. 24365–24398, Apr. 2021, doi: 10.1007/s11042-021-10707-4.

[7] M. Wei, Q. Wu, H. Ji, J. Wang, T. Lyu, J. Liu, and L. Zhao, "A skin disease classification model based on DenseNet and ConvNeXt fusion," *Electronics*, vol. 12, no. 2, p. 438, Jan. 2023, doi: 10.3390/electronics12020438.

[8] C. Hu, B. B. Sapkota, J. A. Thomasson, and M. V. Bagavathiannan, "Influence of image quality and light consistency on the performance of convolutional neural networks for weed mapping," *Remote Sens.*, vol. 13, no. 11, p. 2140, May 2021, doi: 10.3390/rs13112140.

[9] F. Xing and L. Yang, "Robust nucleus/cell detection and segmentation in digital pathology and microscopy images: A comprehensive review," *IEEE Rev. Biomed. Eng.*, vol. 9, pp. 234–263, 2016, doi: 10.1109/RBME.2016.2515127.

[10] L. Rudnicka, M. Olszewska, A. Rakowska, E. Kowalska-Oledzka, and M. Slowinska, "Trichoscopy: A new method for diagnosing hair loss," Tech. Rep., 2008.

[11] Y. LeCun, Y. Bengio, and G. Hinton, "Deep learning," *Nature*, vol. 521, no. 7553, pp. 436–444, May 2015, doi: 10.1038/nature14539.

[12] T. Gebru, J. Morgenstern, B. Vecchione, J. W. Vaughan, H. Wallach, H. D. Iii, and K. Crawford, "Datasheets for datasets," *Commun. ACM*, vol. 64, no. 12, pp. 86–92, Dec. 2021, doi: 10.1145/3458723.

[13] Z. Obermeyer and E. J. Emanuel, "Predicting the future—Big data, machine learning, and clinical medicine," *New England J. Med.*, vol. 375, no. 13, pp. 1216–1219, Sep. 2016, doi: 10.1056/nejmp1606181.

[14] N. Dalal and B. Triggs, "Histograms of oriented gradients for human detection," in *Proc. IEEE Comput. Soc. Conf. Comput. Vis. Pattern Recognit. (CVPR)*, vol. 1, Sep. 2005, pp. 886–893, doi: 10.1109/CVPR.2005.177.

[15] K. He, X. Zhang, S. Ren, and J. Sun, "Deep residual learning for image recognition," in *Proc. IEEE Conf. Comput. Vis. Pattern Recognit. (CVPR)*, Jun. 2016, pp. 770–778, doi: 10.1109/CVPR.2016.90.

[16] E. A. Olsen and D. Canfield, "SALT II: A new take on the severity of alopecia tool (SALT) for determining percentage scalp hair loss," *J. Amer. Acad. Dermatol.*, vol. 75, no. 6, pp. 1268–1270, Dec. 2016, doi: 10.1016/j.jaad.2016.08.042.

[17] E. Bernardis and L. Castelo-Soccio, "Quantifying alopecia areata via texture analysis to automate the SALT score computation," *J. Investigative Dermatol. Symp. Proc.*, vol. 19, no. 1, pp. S34–S40, Jan. 2018, doi: 10.1016/j.jisp.2017.10.010.

[18] S. Lee, J. W. Lee, S. J. Choe, S. Yang, S. B. Koh, Y. S. Ahn, and W.-S. Lee, "Clinically applicable deep learning framework for measurement of the extent of hair loss in patients with alopecia areata," *JAMA Dermatol.*, vol. 156, no. 9, p. 1018, Sep. 2020, doi: 10.1001/jamadermatol.2020.2188.

[19] M. K. Chaitanya, L. D. Sharma, J. Rahul, D. Sharma, and A. Roy, "Artificial intelligence based approach for categorization of COVID-19 ECG images in presence of other cardiovascular disorders," *Biomed. Phys. Eng. Exp.*, vol. 9, no. 3, May 2023, Art. no. 035012.

[20] S. Seo and J. Park, "Trichoscopy of alopecia areata: Hair loss feature extraction and computation using grid line selection and eigenvalue," *Comput. Math. Methods Med.*, vol. 2020, pp. 1–9, Sep. 2020, doi: 10.1155/2020/6908018.

[21] P.-K. Hung, T. W. Chu, R.-Y. Tsai, C.-W. Kung, S.-J. Lin, and C.-M. Chen, "Quantitative assessment of female pattern hair loss," *Dermatolog. Sinica*, vol. 33, no. 3, pp. 142–145, Sep. 2015, doi: 10.1016/j.dsi.2015.01.002.
[22] E. Ludwig, "Classification of the types of androgenetic alopecia (common baldness) occurring in the female sex," *Brit. J. Dermatology*, vol. 97, no. 3, pp. 247–254, Sep. 1977, doi: 10.1111/j.1365-2133.1977.tb15179.x.
[23] R. Savin, "A method for visually describing and quantitating hair loss in male pattern baldness," *J. Investigative Dermatol.*, vol. 98, no. 4, p. 604, 1992.
[24] S.-H. Lee and C.-S. Yang, "An intelligent hair and scalp analysis system using camera sensors and Norwood–Hamilton model," *Int. J. Innov. Comput. Inf. Control*, vol. 14, no. 2, pp. 503–518, 2018.
[25] O. T. Norwood, "Male pattern baldness: Classification and incidence," *Southern Med. J.*, vol. 68, no. 11, pp. 1359–1365, Nov. 1975, doi: 10.1097/00007611-197511000-00009.
[26] H. Benhabiles, K. Hammoudi, Z. Yang, F. Windal, M. Melkemi, F. Dornaika, and I. Arganda-Carreras, "Deep learning based detection of hair loss levels from facial images," in *Proc. 9th Int. Conf. Image Process. Theory, Tools Appl. (IPTA)*, Nov. 2019, pp. 1–6, doi: 10.1109/IPTA.2019.8936122.
[27] C. S. Shakeel, S. J. Khan, B. Chaudhry, S. F. Aijaz, and U. Hassan, "Classification framework for healthy hairs and alopecia areata: A machine learning (ML) approach," *Comput. Math. Methods Med.*, vol. 2021, pp. 1–10, Aug. 2021, doi: 10.1155/2021/1102083.
[28] G. Rai, Naveen, S. Sharma, A. Ansari, and N. Khanduja, "An approach to detect alopecia areata hair disease using deep learning," in *Proc. 6th Int. Conf. Recent Trends Comput.*, Cham, Switzerland: Springer, 2021, pp. 775–783.
[29] S. Aditya, S. Sidhu, and M. Kanchana, "Prediction of alopecia areata using machine learning techniques," in *Proc. IEEE Int. Conf. Data Sci. Inf. Syst. (ICDSIS)*, Jul. 2022, pp. 1–6.
[30] C. Saraswathi and B. Pushpa, "FRCNN based deep learning for identification and classification of alopecia areata," in *Proc. 5th Int. Conf. Electr., Comput. Commun. Technol. (ICECCT)*, vol. 34, Feb. 2023, pp. 1–7.
[31] C. Saraswathi and B. Pushpa, "Machine learning algorithm for classification of alopecia areata from human scalp hair images," in *Proc. ICCVBIC*. Cham, Switzerland: Springer, 2023, pp. 269–288.
[32] A. Mittal, D. B. Biswas, and U. Karthikeyan, "Prediction of alopecia areata using CNN," in *Proc. 2nd Int. Conf. Appl. Artif. Intell. Comput. (ICAAIC)*, May 2023, pp. 141–144.
[33] S. Sayyad and F. Sayyad, "Artificial neural networks algorithms for prediction of human hair loss related autoimmune disorder problem," *J. Auto. Intell.*, vol. 6, no. 2, p. 606, Jul. 2023, doi: 10.32629/jai.v6i2.606.
[34] B. Koonce, "ResNet 50," in *Convolutional Neural Networks with Swift for Tensorflow: Image Recognition and Dataset Categorization*, 2021, pp. 63–72.
[35] M. Raghu, J. Kleinberg, C. Zhang, and S. Bengio, "Transfusion: Understanding transfer learning for medical imaging," in *Proc. Adv. Neural Inf. Process. Syst.*, 2019, pp. 3347–3357.
[36] F. Chollet, "Xception: Deep learning with depthwise separable convolutions," in *Proc. IEEE Conf. Comput. Vis. Pattern Recognit. (CVPR)*, Jul. 2017, pp. 1800–1807, doi: 10.1109/CVPR.2017.195.
[37] F. N. Iandola, S. Han, M. W. Moskewicz, K. Ashraf, W. J. Dally, and K. Keutzer, "SqueezeNet: AlexNet-level accuracy with 50x fewer parameters and <0.5MB model size," 2016, *arXiv:1602.07360*.
[38] M. D. Zeiler and R. Fergus, "Visualizing and understanding convolutional networks," 2013, *arXiv:1311.2901*.
[39] G. Huang, Z. Liu, L. Van Der Maaten, and K. Q. Weinberger, "Densely connected convolutional networks," in *Proc. IEEE Conf. Comput. Vis. Pattern Recognit. (CVPR)*, Jul. 2017, pp. 2261–2269, doi: 10.1109/CVPR.2017.243.
[40] A. Esteva, B. Kuprel, R. A. Novoa, J. Ko, S. M. Swetter, H. M. Blau, and S. Thrun, "Dermatologist-level classification of skin cancer with deep neural networks," *Nature*, vol. 542, no. 7639, pp. 115–118, Feb. 2017, doi: 10.1038/nature21056.
[41] E. Cengil and A. Çinar, "Multiple classification of flower images using transfer learning," in *Proc. Int. Artif. Intell. Data Process. Symp. (IDAP)*, Sep. 2019, pp. 1–6.
[42] G. Litjens, T. Kooi, B. E. Bejnordi, A. A. A. Setio, F. Ciompi, M. Ghafoorian, J. A. W. M. van der Laak, B. van Ginneken, and C. I. Sánchez, "A survey on deep learning in medical image analysis," *Med. Image Anal.*, vol. 42, pp. 60–88, Dec. 2017, doi: 10.1016/j.media.2017.07.005.
[43] H. Abdi and L. J. Williams, "Principal component analysis," *Wiley Interdiscipl. Rev., Comput. Statist.*, vol. 2, no. 4, pp. 433–459, 2010.
[44] S. Wold, K. Esbensen, and P. Geladi, "Principal component analysis," *Chemometrics Intell. Lab. Syst.*, vol. 2, nos. 1–3, pp. 37–52, 1987.
[45] *Figaro 1K*. [Online]. Available: http://projects.i-ctm.eu/it/progetto/figaro-1k
[46] *Dermnet*. [Online]. Available: https://www.kaggle.com/datasets/shubhamgoel27/dermnet
[47] H. Inoue, "Data augmentation by pairing samples for images classification," 2018, *arXiv:1801.02929*.
[48] *Hair Diseases*. [Online]. Available: https://www.kaggle.com/datasets/sundarannamalai/hair-diseases

HAIDER ALI KHAN received the M.S. degree in computer science from Virtual University, Pakistan, in 2019. He is currently pursuing the Ph.D. degree with the Department of Computer Science, University of Engineering and Technology at Taxila, Pakistan. His areas of research interests include computer vision and machine learning.

SYED M. ADNAN received the M.S. degree in computer engineering from the Center for Advanced Studies in Engineering (CASE), Islamabad, Pakistan, in 2010, and the Ph.D. degree in computer engineering from the University of Engineering and Technology at Taxila, Pakistan, in 2014.

Currently, he is an Assistant Professor with the Department of Computer Science, UET Taxila. His areas of research interests include acoustic scene analysis, multimedia signal processing, computer vision, and machine learning.